Proceedings of the ASME 2016 Conference on Smart Materials, Adaptive Structures and Intelligent Systems
SMASIS2016
September 28-30, 2016, Stowe, VT, USA

SMASIS2016-9210

ALULA-INSPIRED LEADING EDGE DEVICE FOR LOW REYNOLDS NUMBER FLIGHT

Boris A. Mandadzhiev *

Graduate Research Assistant
Bio-inspired Adaptive Morphology Lab
Department of Mechanical Engineering
University of Illinois Urbana-Champaign
Urbana, Illinois 61801
Email: mandadz2@illinois.edu

Leonardo P. Chamorro

Assistant Professor

Mechanical Science and Engineering Department
Email: lpchamo@illinois.edu

Michael K. Lynch

Graduate Research Assistant Bio-inspired Adaptive Morphology Lab Email: mklynch3@illinois.edu

Aimy A. Wissa

Assistant Professor

Mechanical Science and Engineering Department
Bio-inspired Adaptive Morphology Lab
Email: awissa@illinois.edu

ABSTRACT

Robust and predictable aerodynamic performance of unmanned aerial vehicles at the limits of their design envelope is critical for safety and mission adaptability. In order for a fixed wing aircraft to maintain the lift necessary for sustained flight at very low speeds and large angles of attack (AoA), the wing shape has to change. This is often achieved by using deployable aerodynamic surfaces, such as flaps or slats, from the wing leading or trailing edges. In nature, one such device is a feathered structure on birds' wings called the alula. The span of the alula is 5% to 20% of the wing and is attached to the first digit of the wing. The goal of the current study is to understand the aerodynamic effects of the alula on wing performance. A series of wind tunnel experiments are performed to quantify the effect of various alula deployment parameters on the aerodynamic per-

formance of a cambered airfoil (S1223). A full wind tunnel span wing, with a single alula located at the wing mid-span is tested under uniform low-turbulence flow at three Reynolds numbers, Re = 85,000, 106,00 and 146,000. An experimental matrix is developed to find the range of effectiveness of an alula-type device. The alula relative angle of attack measured measured from the mean chord of the airfoil is varied to modulate tip-vortex strength, while the alula deflection is varied to modulate the distance of the tip vortex to the wing surface. Lift and drag forces were measured using a six axis force transducer. The lift and drag coefficients showed the greatest sensitivity to the the alula relative angle of attack, increasing the normalized lift coefficient by as much as 80%. Improvements in lift are strongly correlated to higher alula angle, with $\beta = 0^{\circ} - 5^{\circ}$, while reduction in the drag coefficient is observed with higher alula tip deflection ratios and lower β angles. Results show that, as the wing angle of attack and Reynolds number are increased, the overall lift co-

 $^{^{\}ast}\text{Address}$ all correspondence related to ASME style format and figures to this author.

efficient improvement is diminished while the reduction in drag coefficient is higher.

Nomenclature

- α Wing angle of attack (AoA)
- \mathcal{R} Wing aspect ratio
- β Alula chord relative angle to wing chord line
- ε_{sb} Solid blockage
- ρ Density of air
- b Wing span
- b_A Alula span
- C Wind tunnel cross section
- c Wing chord length
- c_A Alula chord length
- C_p Pressure coefficient
- h_A Alula deflection
- K_1 Test article volume
- L_w Lift generated by wing
- L_{wa} Lift from wing with alula deployed
- p_0 Total pressure
- p_1 Static pressure
- q_{∞} Flow dynamic pressure
- Re Reynolds number
- S Wing surface area
- V_{∞} Freestream velocity

1 INTRODUCTION

Life has been evolving for millions of years, adapting to the environment and specializing in ecological niches. Examples of such morphological adaptation are ubiquitous. Swimming and flying require special physiological apparatus, such as leading edge (LE) devices on marine mammals' flippers and on birds' wings, that allow for efficient and versatile operation. Morphology differs between species but generally employs vortex generation techniques to achieve various performance enhancements. Tubercles on the flippers of the humpback whales, for instance, act as passive-flow control structures which modify the flow over the flipper to delay stall and increase the effective span [1-3]. There are many examples of unique physiological characteristics which birds have developed including elliptical wings, short or long wing hands, covert feathers, etc. [4]. The alula is one of such distinguishable devices utilized by birds to improve their flight capabilities. It is a small wing-like structure (Fig.1) located between the hand wing and the arm wing. The Alula is usually covered by 2-6 remiges and is attached to the first digit bone (Fig.1(c)) [5]. Unlike fixed wing aerial vehicles, birds use and adapt their entire bodies for the successful performance of the maneuver or task at hand. Taking off and landing, maneuvering or catching prey, each require unique aerodynamic capabilities. When landing, for instance, the bird enters a controlled descent,

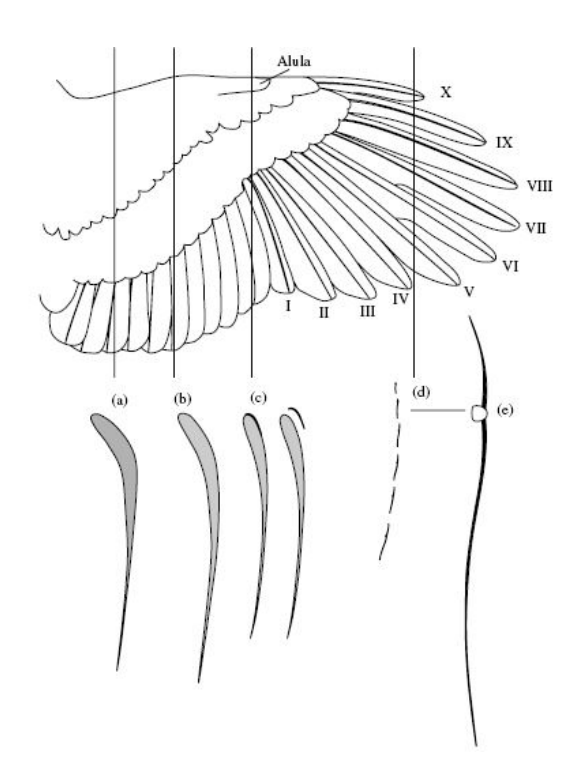


FIGURE 1: Details of dorsal side of a goshawk wing. Five cross sections [a-e] give better understanding of how the wing changes shape. Alula is shown and cross section [c] details its position. Adapted from Videler [5].

continuously reducing its speed. However, since the lift generated by the bird's wings has to equal its weight, the wings' angle of attack (AoA) has to be increased. Immediately before the end of the maneuver, the AoA exceeds the stall angle, and the wing may lose its ability to generate lift [6]. For such a maneuver to be executed in a controlled manner, a stall prevention device such as the alula is essential.

The alula affect the air flow in two ways. The first is through modifying the boundary layer around the wing leading edge, increasing the capacity of the airfoil to sustain higher pressure gradients. This effect is similar to a leading edge slotted flap of a fixed wing aircraft. Traditional leading edge devices, such as slots and flaps, reduce the magnitude of the LE pressure gradient, delaying flow separation at high angles of attack [7,8]. Slots have been shown to increase the maximum lift coefficient of a wing by 37% and delay the stall angle by 24° [8–10]. As described by Abbot and Doenhoff [8], a good boundary layer control device can delay separation of both leading edge laminar flow as well as aft turbulent flow. Another effect of the alula is in the generation of a streamwise tip-vortex. The tip vortices generated by at the alula tips impinge the boundary layer, injecting momentum and delaying flow reversal at steep angles of attack. These two effects

can be classified as a 2D slot effect and as 3D tip vortex generation. A good understanding of these coexisting aerodynamic effects will enable better design of such leading edge devices, which can lead to lower take-off and landing speeds as well as higher maneuverability.

2 PREVIOUS WORK

2.1 ALULA AERODYNAMICS AND BIRD FLIGHT

A few studies have been conducted to unravel the function of the alula and its aerodynamic effects [11–14]. These studies used a combination of PIV (Particle Image Velocimetry), lift-drag measurements, hot-wire anemometry and other methods to quantify birds' wing performance and limitations. The majority of reported investigations are conducted on wither live birds or just bird wings. Aerodynamic testing often requires long and exhaustive experimental matrices, often resulting in deterioration of the test specimen, which means that the results should be interpreted with caution.

The alula is present in a vast number of bird species, attesting to its usefulness and performance gains it delivers. This fact is supported by many experimental and numerical investigations. Test results by Lee *et.al* showed that when the alula is deployed, the wing of the adult male magpies generates $\sim 1-12\%$ more lift and delays stall by $\sim 5-10^{\circ}$ [13]. Furthermore, Austin and Anderson [12] showed that the Lesser Scaup had a 10% increase in lift

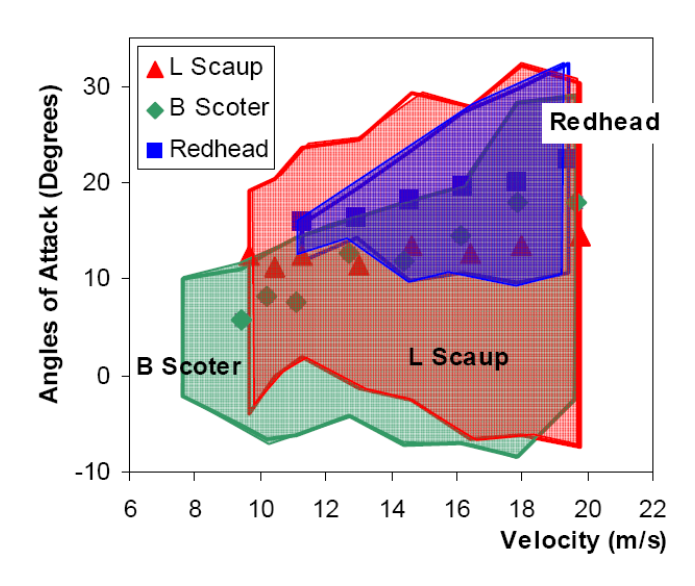


FIGURE 2: Alula deployment envelope. Data points indicate AoA for maximum alula deflection. A trend can be observed in which the AoA at which maximum deflection occurs increases with higher velocities. Also, the minimum AoA for alula deflection decreases for an increase in velocity. Adapted from Austin and Anderson [12].

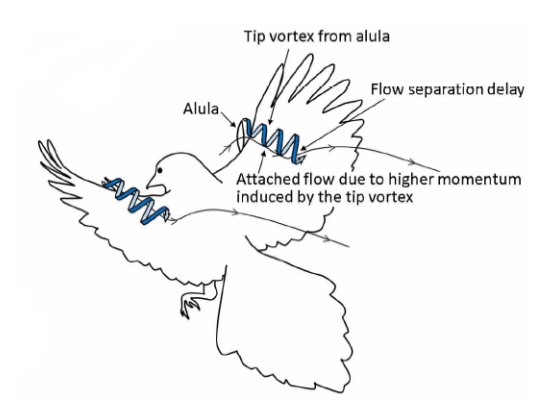


FIGURE 3: Counter-rotating tip vortex formation from alula tips. Adapted from Lee *et al.* [13]

when the alula deflected. They tested the wings at various flow speeds ranging from 7 to 20 m s⁻¹ and AoA from -10° to 35°. They found that in all the three tested birds: the Wood Duck, the Black Scoter and the Lesser Scaup, the alula deflected at a specific velocity and AoA. Figure 2 shows that the alula deflection envelope increases in relation to AoA and the flow velocity. An interesting observation is that the alula deflects at a specific combination of velocity and AoA but then after a certain maximum AoA and velocity it closes again. In Fig.2, Austin and Anderson indicated the maximum alula deflection conditions with a data point. Between the initial alula deployment and closure, there is a constant deflection angle increase as the flow velocity increases. PIV results indicate that the flow behind the wing with the alula deployed is faster and always non-reversed [12]. Even though in the tests with the alula not deployed, the average flow velocity field is non-recirculatory, inspection of the instantaneous velocity field images show areas with flow reversal [12]. This may suggest that the effect of the alula may also lay in its ability to reduce stall risk in addition to being a lift enhancing device.

Lee *et al.* [13] conducted a series of experiments to better understand the aerodynamics of a wing with an alula. They concluded that, when deployed, the alula remiges create a set of counter-rotating vortices moving downstream (Fig.3). The shear layer thickness over the top surface of the wing is decreased by the faster streamwise flow from the downwash flow vector created by the alula tip vortices [13]. The thinner shear layer causes delayed flow separation over the top of the bird wings from the vicinity of the alula towards the wing tips. Furthermore, as the main wing AoA increases, the alula tip distance from the wing LE increases. This mechanism prevents the wing from losing its circulation due to viscous dissipation near the LE surface [13].

Lee *et al.* [13] measured the relative angle between alula and wing chord lines to be -29°, suggesting that the alula does not generate lift at low AoA of the main wing [13]. Only at extreme wing AoA, the alula relative AoA to the freestream is high

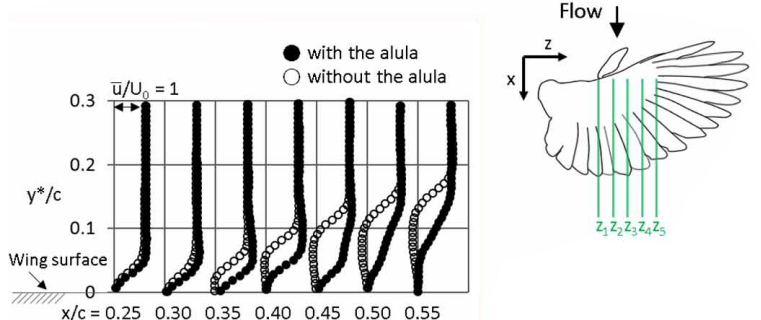


FIGURE 4: Wing upper surface boundary layer velocity profiles at location Z2, with alula - solid circles, without alula - hollow circles. Wing AoA is 24°. Speed is plotted on the vertical axis and is normalized to the mean free-stream velocity of 3 m/s. Horizontal axis is normalized to the chord length of the wing and the data points run to the location where boundary layer flow reversal begins. Adapted from Lee *et al.* [13].

enough to generate strong tip vortex, imparting sufficient momentum on the suction side of the wing [13]. This agrees with test results of leading edge slot devices on fixed airfoils where the slot chord angle of -25° to -35° provides the bulk of the performance increase, and further angle increases results in marginal improvements [9]. Furthermore, the rotation of the streamwise tip vortex induces spanwise velocity over the wing in the distal direction. In Fig.4, the boundary layer velocity profile with the alula deployed shows a delayed flow reversal compared to the clean wing. This mechanism suppresses the flow separation further and is more pronounced in the regions outside of the alula wing tip [13].

2.2 THE EFFECT OF ADAPTATION ON WING MOR-PHOLOGY AND ALULA GEOMETRIC PARAME-TERS

Alvarez *et al.* [11], Crowford and Greenwalt [15], Savile [16] and Norber [17] have studied the flight of a number bird species. Norberg [17] discusses bird morphological flight parameters such as mass, length and area [17]. The derived parameters, aspect ratio (\mathcal{R}) and wing loading (W), are correlated to wing morphology, and a link to the adaptive functions is drawn. Based on form and function, wings are classified in four different types, Class A through D, as shown in Fig.5 [11,16–19]. Important functional relationships between alula size, position, \mathcal{R} and W are reported in references [16] and [11]. Class A birds, such as the *Kingfisher, Common Blackbird and Goldfinches*, are efficient at low to moderate speeds. Their elliptical wings generate elliptical lift distribution and smooth tip vortices, suitable for living in forests and confined spaces [11]. With low to medium W and good flight control, they are adapted to frequent take offs,

landings and accurate maneuverability.

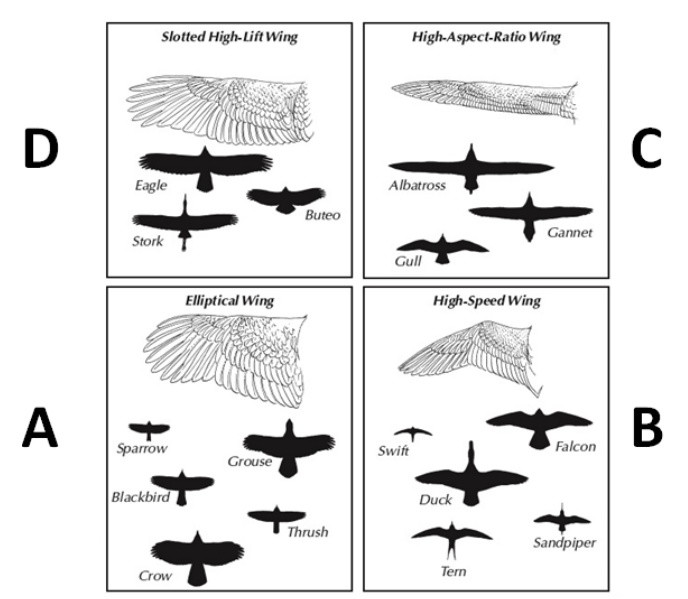


FIGURE 5: Bird wing types based on their morphology and adaptation. Adapted from [20].

Class B are high speed wings of migratory birds or birds of open spaces such as the *Swallow, Dove and Kestrel*. Their wings are characterized by low camber, moderate to high \mathcal{R} and pronounced sweepback. *The Seagull and the Albatross* belong to class C with high AR, high speed wings. They are mainly adapted to flight over water surfaces and well suited for dynamic soaring [11]. Class D birds (*Owls, Storks*) generally have high lift, moderate aspect ratio wings. Their wing tips are slotted and usually have an alula, making them very efficient at low speeds and static soaring over land [11].

Meseguer *et al.* [21] concluded that the alula plays an important role in the flight of birds with higher frequency of take offs and landings and who require good maneuverability. This is supported by the fact that the relative length of the alula to the length of the wing decreases with higher wing AR. The length of the alula is also correlated with the wing loading - low wing loading corresponds to shorter alulae. For example, high wing loading, slow flying birds (i.e. class D birds) require higher lift and better stall control as compared to the moderate and high speed fliers in class B and C.

In summary, the alula is a structure which has evolved to expand the flight envelope capabilities of birds. With no detrimental effect on high speed and gliding flight, it reduces the risk of flow separation at extreme low speeds and AoA. Moreover, the aerodynamics of bird wings with alulae are explored in de-

Bird Specimen	Area S, (cm ²)	Wing Span b, (cm)	Mean Wing Chord c, (cm)	R	Alula Length b_A , (cm)	Mean A Chord (cm)	lula c_A ,	Alula Æ
Test Wing	171.3	44.0	8.0	5.5	6.7	1.9		3.6
Black Scoter	206.5	63.5	11.4	5.56	5.1	1.5		3.4
Lesser Scaup	180.6	53.3	9.5	5.60	3.8	1.0		3.8
Redhead Duck	240.0	61.0	11.1	5.40	5.1	1.5		3.4

TABLE 1: Wing and alula \mathcal{R} were selected to be close to the bird wings to observe similar aerodynamic behavior. Wing measurements of bird species are taken from [12].

tail [12–14], however, research is lacking in describing the effects of varying morphological parameters of the alula on aerodynamic performance. The goal of this study is to provide insight into the flow around a low Reynolds number, high-lift airfoil near stall regimes equipped with an alula-type device. Varying geometrical parameters (relative AoA and deflection) of this device allows for a better understanding of the aerodynamics and the relative effect on the performance of the airfoils. Expanding the knowledge of such a device will assist in the design of low *Re* unmanned aerial vehicles (UAVs) with higher mission adaptability and an extended flight mission envelope.

The paper is organized in six sections. In section 3, a detailed description of the experimental setup and testing schedule is provided. The results, trend analysis and physical phenomena are presented and discussed in section 4. The importance of the results in the design of low-Reynolds number UAVs with wide flight envelope requirements are also discussed. In conclusion, we summarize our findings and provide recommendations for further research.

3 EXPERIMENTAL SETUP

In this work, the alula geometrical parameters that affect the flow over a wing are experimentally investigated. The test parameters are wind speed, wing angle of attack, alula tip deflection and alula angle. Lift and drag force measurements are collected in order to quantify the aerodynamic effect of an alula-like device mounted on an airfoil in post stall conditions.

3.1 WING GEOMETRY AND WIND TUNNEL TEST SET UP

The wing airfoil section and AR used for the experimental matrix are based on previous studies of bird wing shapes and morphological parameters. Table 1 shows a comparison between the tested wing section and bird wing sections presented in the literature [11, 12, 22, 23].

Furthermore, Liu et al. [24] performed a non-contact surface measurement on bird wings using a three-dimensional laser scanner. The inspiration for the wing geometry used in this study stems from the wing planform characteristics, shown in Table 1, and the cross sectional airfoil studies presented in Fig.6 [14, 24, 25]. As a result the high-lift, low-Reynolds number airfoil section, S1223, is selected for this experimental setup. The S1223 camber line and thickness coordinates are similar to the ones of the seagull and merganser (Fig.6) [24]. Figure 6(b) compares the top and bottom wing surface pressure coefficient distributions, and it can be noted that the suction peak and pressure recovery region are comparable. This similarity is important for aerodynamic performance analysis and to further improve the understanding of the alula effect. For a detailed comparison of chord and camber line wing distributions of various birds, one can refer to Liu et al. [24].

The experiments are run in an open-loop wind tunnel at the University of Illinois Urbana-Champaign. There are 4, equal length test sections with variable cross-section areas. To minimize streamwise pressure gradient (dp/dx) the four sections have continuously expanding areas. The first test section is chosen for this experiment due to the low boundary layer thickness and turbulence levels (0.1%). The test specimen profile selected, the S1223, is a well known airfoil for high lift remote controlled competition airplanes. The S1223 has maximum thickness ratio (t/c%) of 12.1% at 19.8% chord and a maximum camber of 8.1% at 49% chord. The test wing chord length (c), is 0.08 m and span (b) - 0.44 m. The wind tunnel test section has a rectangular shape with dimensions: 0.9 m by 0.45 m. Based on the chord length, the test velocity range was selected to produce Reynolds numbers in the range of Re = 80,000 - 150,000, which is representative of birds' and some UAVs' flight. The alula-inspired device span and chord are 67.5 mm and 18.7 mm, respectively. The alula device makes up 15% of the total wing span. Figure 7(a) shows the wing and alula setup in frontal view with the alula tip deflection parameter indicated by h_A . The alula relative angle

of attack, β , is shown in a cross sectional side view of the setup in Fig.7(b).

Solid and wake blockage effects have been considered and calculated in order to verify their effect is minimal and will not distort test results. Solid and wake blockage effects modify the flowfield in the vicinity of the test airfoil by the presence of test section walls. Buoyancy effects have not been considered due to the absence of a wind tunnel longitudinal pressure gradient. Formulation for blockage and wake effects are summarized by Burlow, Rae and Pope [26]. The solid blockage increment is computed using the following relationship:

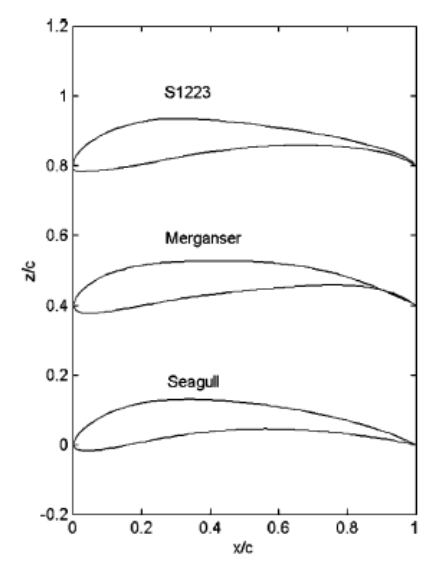
$$\varepsilon_{sb} = K_1/C^{3/2} \tag{1}$$

In Eq.1, K_1 is the model volume and for the test wing specimen, and C is the wind tunnel test section cross sectional area. The solid blockage effect of the test airfoil is found to be 0.1%. Wake blockage effects were also considered, but due to the fact that the airfoil is a streamlined object at relatively shallow angles of attack, the effect is negligible. Furthermore, the trailing vortex system that impinges the boundary layer is weak, and the downwash effect corrections will not be considered [26].

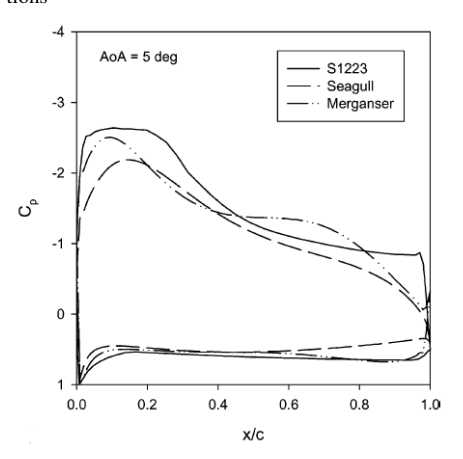
3.2 FORCE MEASUREMENTS

The test airfoil with an alula is mounted to an ATI Gamma 6-axis force/torque sensor with amplified, high-signal-to-noise ratio signal output and a sensitivity of 1/160 N. The sensor axes are aligned with the wind tunnel flow direction and is fixed to the test section ceiling wall. The wing AoA can be set at a maximum value of 40° relative to the free stream flow direction. The airfoil is mounted to an adapter plate, which is firmly attached to the sensor (Fig.8). The desired angle of attack is set by rotating the adapter plate with respect to the sensor axes. In order to decrease the force loading on the +X and +Y axis of the sensor due to aerodynamic forces, the airfoil section is supported by a reaction force at the floor of the test section. The airfoil is free to rotate around a pivot point close to the airfoil quarter chord location, c/4, and is aligned with the centerline of the adapter plate. Velocity at the test location is measured by a static-pitot tube connected to a differential pressure sensor. The differential pressure reading is processed and output in a CSV form by a National Instruments data acquisition unit (NI-DAO). The distance of the static-pitot tube to the leading edge of the wing is five airfoil chord lengths, which results in a velocity correction increment of < 3% [27]. The differential pressure reading is converted to free stream velocity magnitude using Bernoulli's Equation:

$$V_{\infty} = \sqrt{2(p_0 - p_1)/\rho}$$



(a) Comparison between hihgly cambered, high-lift airfoil S1223 to the Seagul and Merganser wing sections



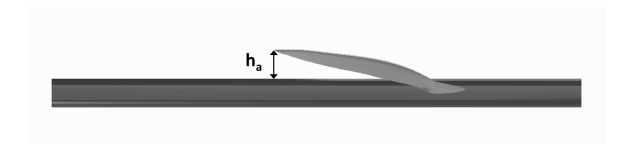
(b) Pressure coefficients on top and bottom airfoil surfaces are comparable.

FIGURE 6: Wing airfoil section comparison between various bird species and a high-lift, low-Reynolds number airfoil S1223. Adapted from [24].

3.3 TEST MATRIX AND DESIGN OF EXPERIMENT

Three Reynolds numbers are selected to study wing performance and alula effectiveness: Re=85,00, Re=106,000, and Re=146,000. The wing angle of attack, α , is varied from 0° to 19° in 2° increments. To test the effect of the alula, a design of experiment (DOE) test matrix is developed for each Re and a fixed α . Table 2 shows the test sequence and run parameters of the four test sets.

The alula angle and tip deflection to alula span ratio are used



(a) Front View showing alula deflection parameter h_A



(b) Side view cross section of test wing and alula, showing alula relative angle, β .

FIGURE 7: Test wing geometry and alula parameters.

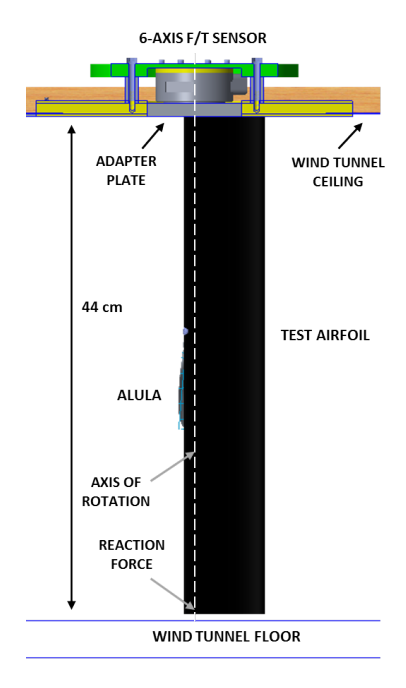


FIGURE 8: Detailed experimental setup schematic.

as the input parameters in the DOE matrix in order to evaluate main effects and interactions between these two parameters at different flow speeds and angles of attack. The test matrix used is a full factorial 3 level design with 2 input parameters and was run in a randomized sequence. Non-normalized alula tip deflections are h_A : 5 mm, 15 mm, 25 mm. Table 3 shows an example of typical DOE matrix used at Re = 106,000 and $\alpha = 10^{\circ}$.

TABLE 2: Four test matrices are developed to test the effect of Re and wing AoA on the performance of the alula. For each DOE matrix Re and α are constant

Parameter	DOE#1	DOE#2	DOE#3	DOE#4	
Re	106,000	106,000	85,000	146,000	
$lpha^\circ$	10	16	8	10	

TABLE 3: Table showing DOE#1 test matrix randomized run sequence with β and h_A/b_A as input parameters $\alpha = 10^{\circ}$, Re = 106,000

Run	1	2	3	4	5	6	7	8	9
β°	-5	-5	0	0	-10	-10	-10	0	5
h_A/b_A	.075	.224	.224	.075	.075	.224	.373	.373	.373

4 RESULTS

The alula feathers are attached to the "thumb" of the wing wrist of the bird, and as such, the control and sensitivity are comparable to other digits. There are inconsistent conclusions made previously as to whether or not the alula is actively or passively deployed. Alvarez et al. [11] tested the hypothesis and found that there is no difference in alula deployment of a bird wing only and a live bird. With only small differences in the alula deflection between the two cases, the onset of alula deflection is similar with respect to flow velocity and angle of attack. This leads to the conclusion that the alula deployment is an involuntary action, a product of high suction peaks near the wing leading edge [11]. However, the alula digit has all muscles and nervous endings for active motion. To further examine the alula management, our experimental setup is designed such that maximum adjustability is achieved. The alula tip deflection from the wing surface is set manually and has a pivot point in its root. The deflection is measured in mm from the wing surface and is reported as a ratio with respect to the alula span, h_A/b_A . The alula chord line angle, β , is measured from the wing chord and is varied between -10° and 5°. In order to normalize the effects of the alula on the overall performance of a wing with an arbitrary shape, the incremental change in lift due to the alula is compared to the lift generated by the relative wing span covered by the alula.

$$\Delta L_A = \frac{L_{wa} - L_w}{b_A b^{-1} L_w} \tag{2}$$

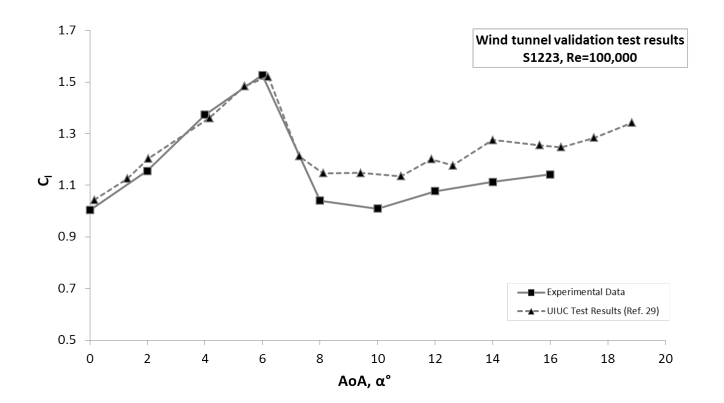
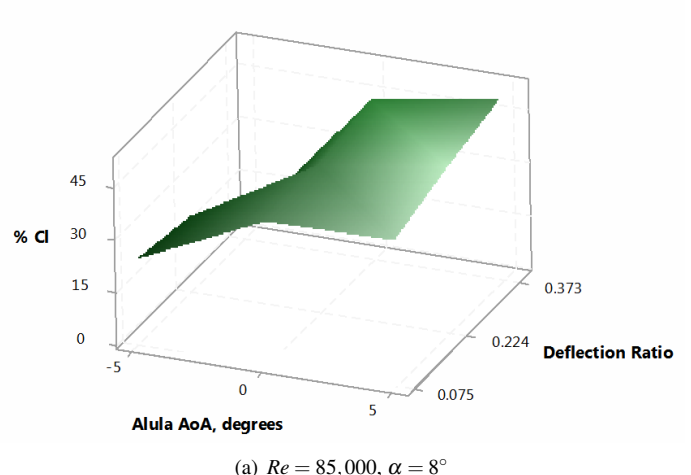


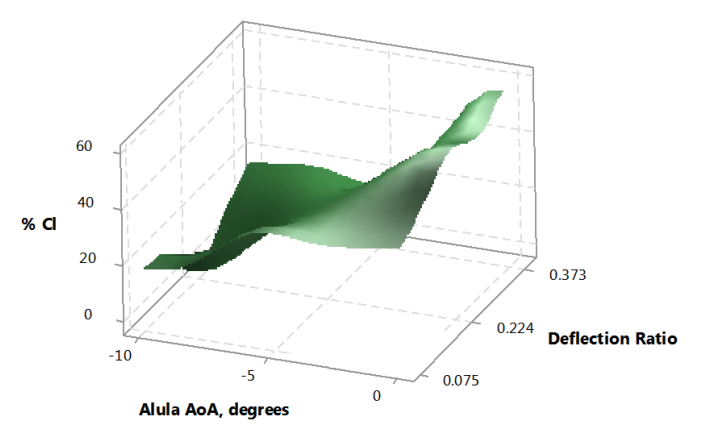
FIGURE 9: S1223 lift curve experimental result validation to previously conducted tests at University of Illinois Urbana-Champaign [28]

Equation 2 shows the expression for the total lift force increment (ΔL_A) produced by the alula normalized by the alula span ratio. L_w is total lift produced by the wing with no alula deployment and at the same aerodynamic conditions, and L_{wa} is the total lift produced by the wing with the alula deployed. Converting to the dimensionless parameter C_l yields the same fractional values as both the numerator and denominator are referenced to $q_{\infty}c_Ab_A$.

4.1 C_l SENSITIVITY TO ALULA ANGLE OF ATTACK, β AND DEFLECTION RATIO, h_A/b_A

The effect of an alula-like leading edge device on the performance of an airfoil, such as the S1223, can be evaluated in a multitude of ways. As mentioned earlier, when the alula is deflected in bird flight, the flow over the wing is modified to sustain higher pressure gradients typical in high angles of attack. In order to eliminate 3D wing effects, the wing is designed to span the entire wind tunnel, eliminating any trailing vortices and in effect, creating an infinite, 2D airfoil. The selected low Reynolds number, high-lift airfoil, the S1223, has been tested previously [28] and lift curves are compared in Fig.9. Figure 10 shows the percent change in the normalized lift coefficient, C_l , at various alula tip deflection ratios, h_A/b_A , and alula relative angles of attack, β . In Fig.10(a), $\alpha = 8^{\circ}$ is selected as the post stall angle since the stall angle of the baseline airfoil is $\alpha = 4^{\circ}$, where in the test cases with Re = 106,000 and Re = 146,000, the post stall angle is selected to be $\alpha = 10^{\circ}$ since airfoil stall occurs at $\alpha = 6^{\circ}$ (Fig.9). At Re = 85,000, the maximum C_l increase is 51.1% at $\beta = 5^{\circ}$ and $h_A/b_A = 0.373$. At Re = 106,000, the highest increase in C_l , 50% to 60%, occurs at $\beta = 0^{\circ}$ and at all deflection ratios. Figure 11(b) shows the large effect the alula angle has on lift generation. At Re = 146,000, maximum improvement is 40.6% and, again, occurs at $\beta = 0^{\circ}$. Furthermore, the only positive changes in C_l are at $\beta = 0^{\circ}$ and all deflection ratios. At $\beta = -10^{\circ}$ and





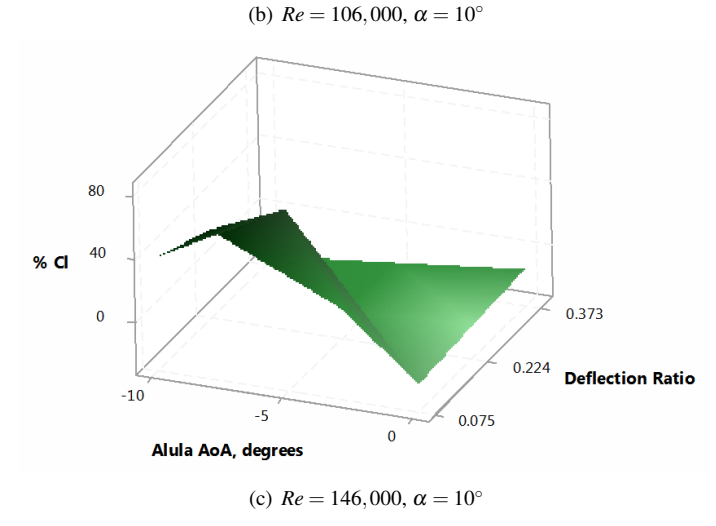


FIGURE 10: Surface plots of β and h_A/b_A on the normalized lift coefficient, C_l

 $h_A/b_A = 0.075$ there is a 21.1% loss of lift, showing that at poor selection of alula parameters, a negative impact in wing performance can be observed.

The alula performed, surprisingly, better at higher alula relative angles of attack. This result can be explained by the larger lift values created by the alula at higher angles of attack, which is needed in order to sustain the alula trailing vortex strength and re-energize the boundary layer on the wing. Small β angles may be favorable to the lift coefficient because of better flow attachment over the alula and hence delayed flow reversal on the top surface of the wing. However, due to the alula sharp leading edge and camber, at small alula angles of attack, bottom surface leading edge separation can occur. This aligns with the trend that the maximum lift increase occurs at the highest alula relative angles. Moreover, in most cases the alula angle of attack had the most influence on the lift coefficient change when compared to the alula tip deflection ratio.

4.2 REYNOLDS NUMBER EFFECTS

In Fig.11 and Fig.12, the relative effect of each variable on the percentage of lift coefficient change and the drag coefficient is compared at each *Re* number. The results show that the alula is effective in improving lift throughout the Re range tested. Moreover, the improvements in lift is most sensitive to variations in alula angle of attack at Re = 106,000. The highest C_l increase (80%) occurs at Re = 146,000 at a single β and h_A/b_A combination. In contrast, C_l shows an increase for all configurations at Re = 85,000, but improvements start to diminish at $\beta < 0^{\circ}$. This can be explained by the fact that, at low speeds, the flow is unable to climb steeper pressure gradients resulting from higher suction peaks near the leading edge. This statement is supported by the sharp increase in C_d after $\beta > 0^\circ$ (Fig.12(a)). At Re = 106,000, C_l increases the most at the highest alula angle of attack, however, the highest alula tip deflection ratio has an adverse affect on the drag coefficient (Fig. 12(b)).

The above results indicate that the alula is more effective over a wider range of angles and deflection ratios at Re = 106,000, but shows a higher lift coefficient increment at a single combination of alula angle and tip deflection ratio at Re = 146,000. In fact, with Re = 146,000 and at off optimal settings, the alula is much less effective as compared to Re = 106,000. At lower speeds, such as Re = 85,000, the lift increase is observed with all combinations of β and h_A/b_A . The lowest increase in C_l is 3.7% while the optimal combination yields 51.1% improvement.

As noted previously, the effect on percent C_l increase over the clean wing results at Re=106,000 is most pronounced. To better understand the physics at this Re, a test matrix at wing AoA $\alpha=16^\circ$ was also completed. Figure 13 and Figure 14 show the effect of α on lift coefficient change. Increasing the angle of attack from 10° to 16° reduces the mean increase in lift from the

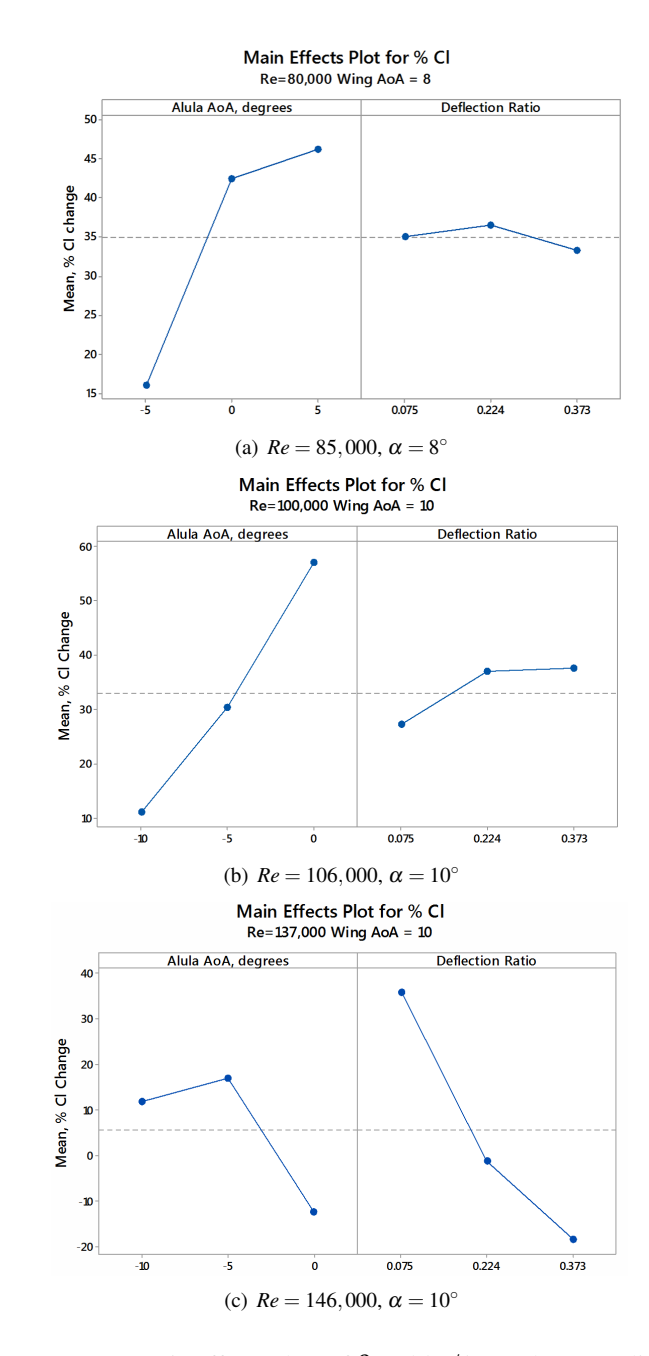


FIGURE 11: Main effects plots of β and h_A/b_A on the normalized lift coefficient, C_l

alula. This result suggests that the separation location on the top surface of the wing becomes more difficult to delay. With higher wing AoA, the C_p peak at the wing leading edge increases, causing faster transition to turbulent flow and subsequently reversal and flow separation. Thus with non-optimal alula setup combinations, flow instabilities and sharp pressure gradients are created,

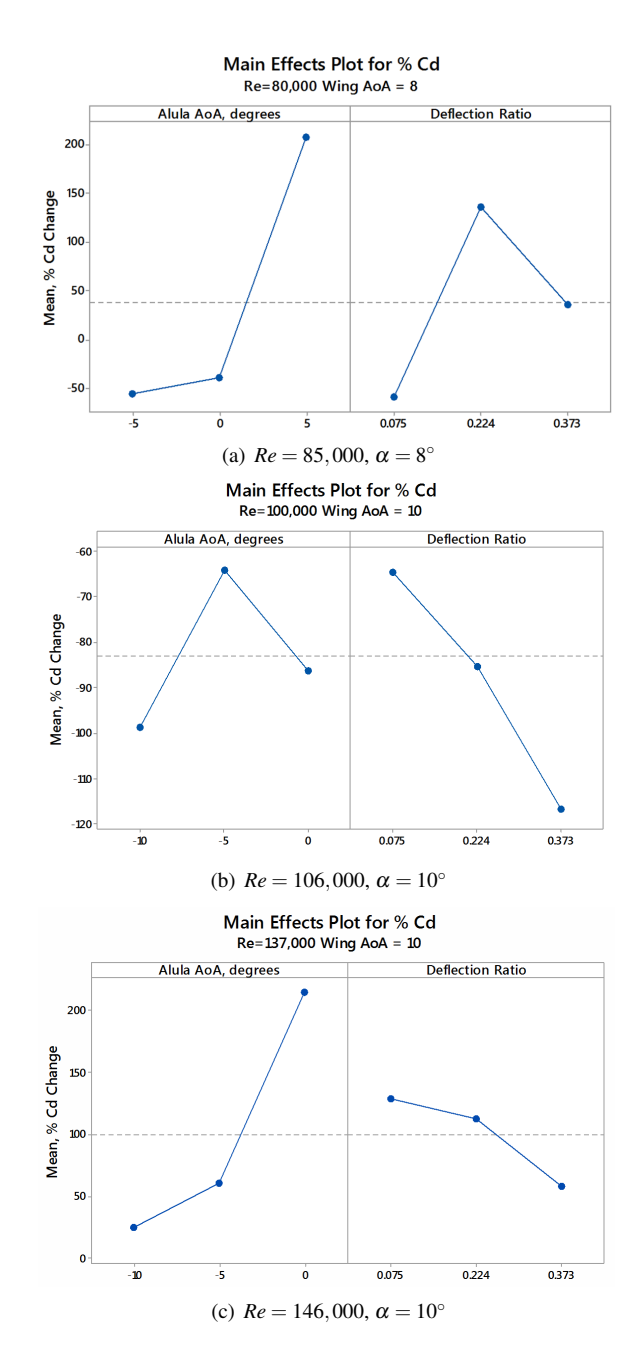


FIGURE 12: Main effects plots of β and h_A/b_A on the normalized drag coefficient, C_d

resulting in significantly decreased and even negative effects on lift generation due to the presence of the alula.

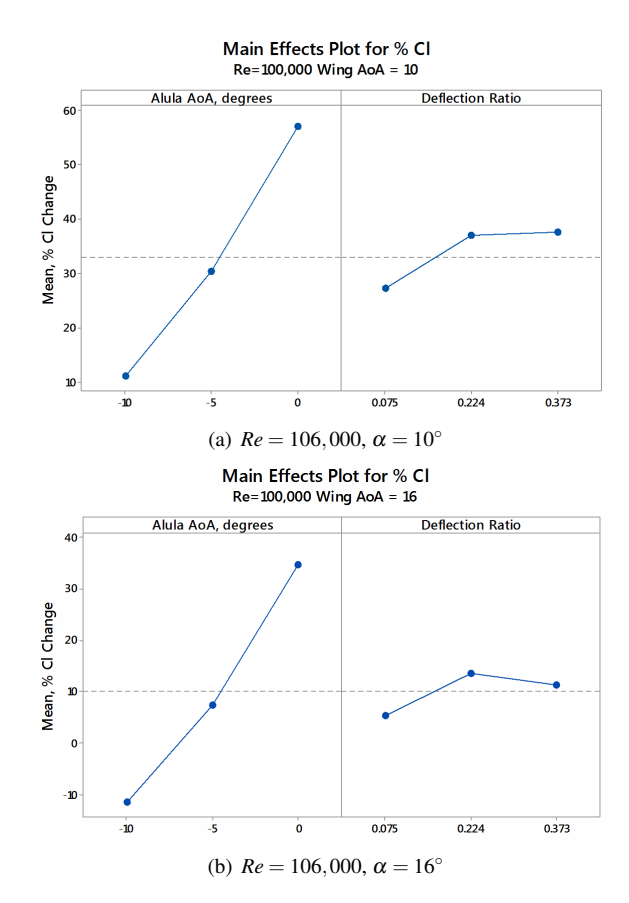


FIGURE 13: Main effects plots of β and h_A/b_A on the percent change in normalized lift coefficient, C_l with two different wing

4.3 ALULA-INSPIRED DEVICES FOR MISSION ADAPTABILITY

The results presented in this work confirm previous findings on the aerodynamic effect of the alula. Significant increases in the lift produced by a wing can be achieved when the alula is deployed at post stall conditions without affecting the aerodynamic performance at cruise conditions. Increasing the lift coefficient of an aerial vehicle has an important impact on takeoff and landing distances, increased maneuverability and improved control. Furthermore, susceptibility of lower mass flying objects to flow instabilities, such as wind gusts, can be significantly mitigated by an alula-inspired device. In the event of a sudden flow direction change or rapid descend the angle of attack may exceed the stall angle causing loss of lift and poor stability. In such instances the alula device will deploy, restoring lift and reattaching flow over control surfaces. Moreover, the aerodynamic efficiency (L/D) of the full span wing increases by as much as 64% with the alula deployed. In most cases the highest L/D ratio is observed with the largest positive lift coefficient increment. When an aircraft

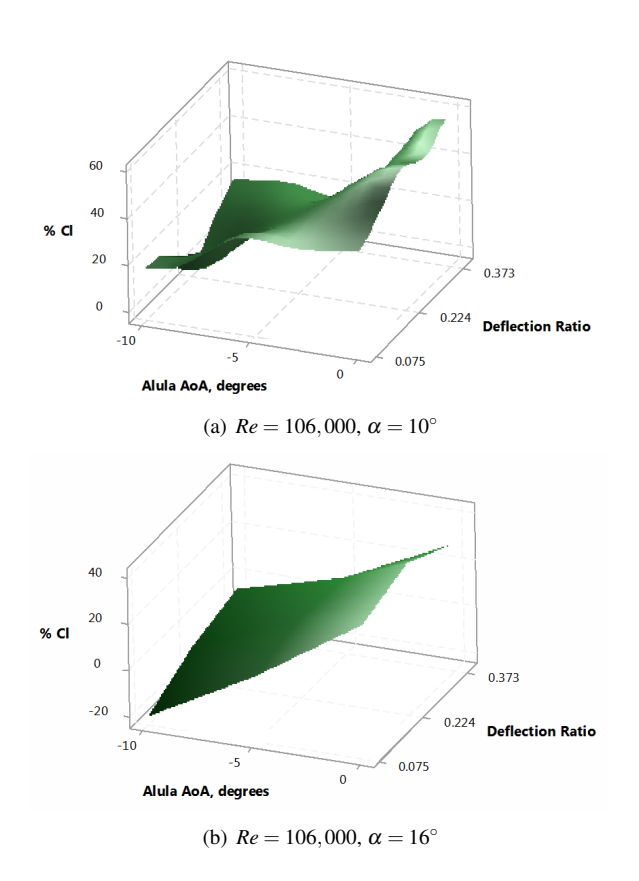


FIGURE 14: Main effects plots of β and h_A/b_A on the percent change in normalized lift coefficient, C_l with two different wing α .

is perching or landing a high L/D ensures smooth and controlled descend, while increased $C_{L_{max}}$ enables lower approach speeds and higher payload capacity. Thus, by modifying the flow around the wing, delaying flow separation and increasing stall angle, the ability of the aircraft to operate in unpredictable and changing environment is significantly improved.

An alula-inspired device can be an integral part in the design of low-Reynolds number UAVs with wide flight envelope requirements. However, the results presented here show that the device performance is very sensitive to a variety of parameters, i.e. Re, AoA, alula angle of attack and deflection ratio. To achieve the desired performance level, these parameters must be tuned for the conditions the aircraft will be operating in. At higher Re the alula provides increase in post stall C_L only at few β and h_A/b_A combinations and has a negative effect in all other configurations. As discussed by Alvarez et al., the high pressure coefficient peak forming at the LE of an airfoil at high angles of attack exerts a force normal to the alula. With a sufficient lift force, the alula separates from the wing LE and rapid deflec-

tion occurs [11]. Because this behavior is identical between live and dead birds, the conclusion can be made that the alula is a passively deployed aerodynamic surface. This makes the alulainspired device suitable for any aircraft design, and in particular small scale and low speed UAVs.

5 CONCLUSION

A test matrix is designed to test and analyze the aerodynamic effect of an alula-inspired leading edge device. The wing airfoil selected is a low-Re, high-lift section, which has similar characteristics to some birds' wings and is used in low Re aircraft design. The tests are run in a low turbulence, constant pressure test section wind tunnel, with wing force measurements used as output parameters. Results show improvement trends in the lift and drag coefficient at the tested Re and α . The lift and drag coefficients showed the greatest sensitivity to the alula relative angle of attack, increasing the normalized lift coefficient by as much as 80% at Re = 146,000, $\beta = -5^{\circ}$ and $h_A/b_A = 0.075$. Improvements in lift are strongly correlated to higher alula incidence angle, with $\beta = -5^{\circ}$ to 5° producing the highest increase in C_l . The largest reduction in the drag coefficient is observed with higher alula tip deflection ratios and lower β angles. Due to the diminishing aerodynamic effect of the alula, increasing the wing angle of attack reduces the improvements in C_l and C_d . Increasing $C_{L_{max}}$, aerodynamic efficiency and reducing drag of an aircraft wing results in higher payload capacities, shorter runways, and improved stability and control. Actively responding to changing flow conditions, the alula device mitigates stall risk and flight instabilities as well. As a passively deployable structure, the weight penalty is minimal while reliability and effectiveness are maximized.

ACKNOWLEDGMENT

The authors acknowledge support from the Mechanical Science and Engineering Department at the University of Illinois Urbana-Champaign. Resources from the Renewable Energy and Turbulent Environment group as well as the Bio-inspired Adaptive Morphology Lab are greatly appreciated.

REFERENCES

- [1] Fish, F. E., Weber, P. W., Murray, M. M., and Howle, L. E., 2011. "The tubercles on humpback whales' flippers: Application of bio-inspired technology". *Integrative and comparative biology*, **51**(1), pp. 203–213.
- [2] Miklosovic, D., Murray, M., Howle, L., and Fish, F., 2004. "Leading-edge tubercles delay stall on humpback whale (megaptera novaeangliae) flippers". *Physics of Fluids* (1994-present), **16**(5), pp. L39–L42.

- [3] Pedro, H. T., and Kobayashi, M. H., 2008. "Numerical study of stall delay on humpback whale flippers". In 46th AIAA aerospace sciences meeting and exhibit, pp. 2008– 0584
- [4] Rayner, J. M., 1988. "Form and function in avian flight". In *Current ornithology*. Springer, pp. 1–66.
- [5] Videler, J. J., 2006. Avian flight. Oxford University Press.
- [6] Anderson Jr, J. D., 1985. *Fundamentals of aerodynamics*. Tata McGraw-Hill Education.
- [7] O. Smith, A., 1975. "High-lift aerodynamics". *Journal of Aircraft*, **12**(6), pp. 501–530.
- [8] Abbott, I. H., and Von Doenhoff, A. E., 1959. *Theory of wing sections, including a summary of airfoil data*. Courier Corporation.
- [9] Weick, F. E., and Platt, R. C., 1933. "Wind-tunnel tests on model wing with fowler flap and specially developed leading-edge slot".
- [10] Weick, F. E., and Bamber, M. J., 1933. "Wind-tunnel tests of a clark y wing with a narrow auxiliary airfoil in different positions".
- [11] Alvarez, J., Meseguer, J., Meseguer, E., and Pérez, A., 2001. "On the role of the alula in the steady flight of birds". *Ardeola*, **48**(2), pp. 161–173.
- [12] Austin, B., and Anderson, A. M., 2007. "The alula and its aerodynamic effect on avian flight". In ASME 2007 International Mechanical Engineering Congress and Exposition, American Society of Mechanical Engineers, pp. 797–806.
- [13] Lee, S.-i., Kim, J., Park, H., Jablonski, P., and Choi, H., 2015. "The function of the alula in avian flight". *Scientific reports*, **5**.
- [14] Nachtigall, P. D. W., and Wieser, J., 1966. "Profilmessungen am taubenflügel". *Zeitschrift für vergleichende Physiologie*, **52**(4), pp. 333–346.
- [15] Greenewalt, C. H., 1975. "The flight of birds: the significant dimensions, their departure from the requirements for dimensional similarity, and the effect on flight aerodynamics of that departure". *Transactions of the American philosophical society*, pp. 1–67.
- [16] Savile, D., 1957. "Adaptive evolution in the avian wing". *Evolution*, pp. 212–224.
- [17] Norberg, U. M., 2012. Vertebrate flight: mechanics, physiology, morphology, ecology and evolution, Vol. 27. Springer Science & Business Media.
- [18] Watts, P., and Fish, F., 2001. "The influence of passive, leading edge tubercles on wing performance". In Proc. Twelfth Intl. Symp. Unmanned Untethered Submers. Technol, Auton. Undersea Syst. Inst. Durham New Hampshire.
- [19] Kokshaysky, N. V., 1973. "Functional aspects of some details of bird wing configuration". *Systematic Biology*, **22**(4), pp. 442–450.
- [20] Podulka, S., Rohrbaugh, R. W., Bonney, R., et al., 2004. *Handbook of bird biology*. Cornell Lab of Ornithology

- Ithaca, New York.
- [21] Meseguer, J., Franchini, S., Pérez-Grande, I., and Sanz, J., 2005. "On the aerodynamics of leading-edge high-lift devices of avian wings". *Proceedings of the Institution of Mechanical Engineers, Part G: Journal of Aerospace Engineering*, **219**(1), pp. 63–68.
- [22] Norberg, U. M., 1979. "Morphology of the wings, legs and tail of three coniferous forest tits, the goldcrest, and the treecreeper in relation to locomotor pattern and feeding station selection". *Philosophical Transactions of the Royal Society of London B: Biological Sciences*, **287**(1019), pp. 131–165.
- [23] Norberg, U. M., 1994. "Wing design, flight performance, and habitat use in bats". *Ecological morphology: integrative organismal biology*, pp. 205–239.
- [24] Liu, T., Kuykendoll, K., Rhew, R., and Jones, S., 2006. "Avian wing geometry and kinematics". *AIAA journal*, **44**(5), pp. 954–963.
- [25] Carruthers, A., Walker, S., Thomas, A., and Taylor, G., 2010. "Aerodynamics of aerofoil sections measured on a free-flying bird". *Proceedings of the Institution of Mechanical Engineers, Part G: Journal of Aerospace Engineering*, **224**(8), pp. 855–864.
- [26] Rae, W. H., and Pope, A., 1984. Low-speed wind tunnel testing. John Wiley.
- [27] Giguere, P., and Selig, M. S., 1997. "Freestream velocity corrections for two-dimensional testing with splitter plates". *AIAA journal*, **35**(7), pp. 1195–1200.
- [28] Selig, M. S., 1995. Summary of low speed airfoil data, Vol. 1. SoarTech.